JOURNAL OF GUIDANCE, CONTROL, AND DYNAMICS
Vol. 24, No. 3, May–June 2001

Category II Pilot in-the-Loop Oscillations Analysis from Robust Stability Methods

Francesco Amato* and Raffaele Iervolino†
University of Naples "Federico II," 80125 Naples, Italy
and
Stefano Scala‡ and Leopoldo Verde§
Centro Italiano Ricerche Aerospaziali, 81043 Capua, Italy

In this paper we deal with the analysis of pilot in-the-loop oscillations (PIO) of category II (with rate or position limiting). We propose an approach, based on robust stability analysis, which assumes that PIOs are characterized by a limit cycle behavior. In this way we obtain two different methods for the analysis of category II PIOs; the first method replaces the nonlinear element (contained in the model of the rate or position limited actuator) by a linear time-invariant gain and is shown to be equivalent to the classical describing function analysis, with the advantage of preventing the computational difficulties of the describing function approach. The analysis via time-invariant gain may be, however, optimistic in predicting PIOs for a given aircraft. Therefore a further method, based on stability analysis via Lur'e Lyapunov functions, is provided; such a method guarantees asymptotic stability of the nonlinear plant and can give conservative results. By the use of both methods, a complete analysis of the nonlinear system can be performed. The X-15 case study is considered to illustrate the effectiveness of the proposed methodology.

I. Introduction

PILOT in-the-looposcillation (PIO) is a well known and sadly famous phenomenon in the field of handling qualities of aircraft, which has been encountered and studied well before the advent of active control technology and fly-by-wire flight control systems (FCS). Its origin is a misadaptation between the pilot and the aircraft during some tasks in which tight closed-loop control of the aircraft is required from the pilot, with the aircraft not responding to pilot commands as expected by the pilot himself. This situation can trigger a pilot action capable of driving the aircraft out of pilot control, which in some cases can only be recovered by the pilot releasing the column and exiting from the control loop.

The introduction of fly-by-wire FCS has in a sense exacerbated the problem of PIOs because the multitude of FCS modes, which can be easily designed and included into the new digital FCS, can very easily disorient the pilot in the interpretation of the aircraft response to his actions. Indeed the three elements that are considered in PIO analysis are the pilot, the aircraft dynamics, and the trigger, an event which can introduce the misadaptation.[1] Examples of the trigger are a mode change or an unexpected nonlinear behavior in the FCS or a variation in the pilot control behavior, such as an increase of the pilot gain. This situation has forced the U.S. military authorities to write down since 1982 explicit flying qualities requirements for PIOs in their Military Standard Specification Documents.[2] An even greater emphasis is given to PIOs detection methods in the new issues of this standard.[3,4]

Because of the highly destructive potential of the PIO phenomenon, a great effort has been spent in the last years in many research programs both in the United States and Europe[1,5–7] to study PIOs, in order to derive methods able to predict the tendency of an aircraft to develop PIOs.

PIO phenomena are commonly divided into three categories depending on the dynamical behavior of the closed-loop pilot-vehicle system, ranging from the linear to the highly nonlinear.

In this paper we focus on category II PIOs, which are mainly characterized by the saturation of position or rate-limited elements. This kind of nonlinearity is unavoidably present in every aircraft because of physical constraints of elements such as stick/column deflections, actuators position and rate limiters, limiters in the controller software, and so on. In particular, rate-limited actuators can expose the pilot to a sudden change of the dynamics of the augmented aircraft (flying qualities cliff) and have been indicated as the concurring cause of various high dramatic PIO incidents/accidents in the last years (YF22, Gripen).

The resulting PIO has the form of a limit cycle of the nonlinear system; thus limit cycle analysis is a sensible way to study the pilot-vehicle closed-loop system in order to predict this kind of PIO.

A classical method for the analysis of category II PIOs is the describing function method. Novel methods have been investigated in the last years: among them the open-loop onset point (see Ref. 8), which derives from the describing function method, the time-domain Neal–Smith method,[9] which translates into the time domain the classical frequency domain Neal–Smith method, and the μ-analysis-based method proposed in Ref. 6.

In this context we shall introduce an alternative method to predict category II PIOs, which is shown to be equivalent to the describing function method. The proposed approach has the potential to prevent the computational difficulties present in the describing function analysis. This new detection method is based on a methodology for robustness analysis of dynamic properties of linear systems subject to time-invariant parameters[10] and is applied, in our case, by replacing the nonlinear element by a constant, but uncertain, parameter. The methodology has been applied in the past with a good success to perform sensitivity analysis of flying qualities with respect to uncertainties of physical parameters of the augmented aircraft.[11,12]

On the other hand, the methodology that tests robust stability vs a time-invariant parameter (and therefore also describing function based methods) may result optimistically in the prediction of PIOs for a given aircraft because stability vs a time-invariant parameter does not guarantee stability if the parameter is time varying (see Ref. 13, Chap. 4), which is the actual situation we deal with because the instantaneous input-output gain of the nonlinear element is time varying.

Presented as Paper 99-4006 at the AIAA Atmospheric Flight Mechanics Conference, Portland, OR, 9–11 August 1999; received 24 January 2000; revision received 13 June 2000; accepted for publication 20 June 2000. Copyright © 2000 by the American Institute of Aeronautics and Astronautics, Inc. All rights reserved.

*Associate Professor, Dipartimento di Informatica e Sistemistica, Via Claudio 21; framato@unina.it.

†Ph.D. in Electrical Engineering, Dipartimento di Informatica e Sistemistica, Via Claudio 21; rafierv@unina.it.

‡Scientist, Flight Systems Department, Via Maiorise; s.scala@cira.it.

§Head, Flight Systems Department, Via Maiorise; l.verde@cira.it.

A possible way to validate robust stability analysis is that of performing exhaustive time simulations of the nonlinear system; however, this approach may be extremely time consuming.

Therefore a further approach, based on a simple analytical technique which leads to a sufficient (conservative) condition for stability, is proposed. Such an approach looks directly at the nonlinear element, and the stability analysis is performed by means of the so-called Lur'e Lyapunov functions (see Ref. 13, Chap. 5). By the use of both analytical methods, a complete analysis of the nonlinear system can be performed.

Finally we recall that a preliminary version of this paper has been presented at the 1999 AIAA Conference in Portland.[14]

II. Problem Description

The formal definition of PIOs given in Ref. 15 is, "There shall be no tendency for pilot-induced oscillations, that is, sustained or uncontrollable oscillations resulting from the efforts of the pilot to control the airplane."

As defined in the MIL specs, PIO is an umbrella under which the same phenomenon (closed-loop pilot-vehicle oscillation) can show very different behaviors, mainly depending on the underlying cause of the PIO occurrence. In the following we recall a classification of PIO[1] that takes into account some possible different behaviors of the closed-loop pilot-vehicle system during the PIO. In the given classification three different behaviors are recognized, leading to three PIO categories:

1) PIO category I—The closed-loop pilot-vehicle system has a linear behavior.

2) PIO category II—The closed-loop pilot-vehicle system has a nonlinear behavior, mainly characterized by the saturation of position or rate limited elements.

3) PIO category III—The closed-loop pilot-vehicle system has a highly nonlinear behavior, with no further peculiar characteristic.

In this paper we focus on category II PIO, for which it is assumed that PIO are characterized by limit cycles of the closed-loop pilot-vehicle system.

Let us refer to the block diagram in Fig. 1, where a classical closed-loop scheme for the study of category II PIO occurrence in the pitch axis is considered. The main blocks in Fig. 1 are the pilot gain K_p, the nonlinear actuator, whose rate limiting is provided by the saturation nonlinearity (normalized to be symmetric with unitary slope) that precedes the position integrator, and the aircraft dynamics transfer function $\theta(s)/\delta(s)$ from the control surface position to the variable controlled by the pilot.

The notation for the normalized nonlinearity with equation

$$y = N(u) \tag{1}$$

is given in Fig. 2. With $y_{\max}$ we denote the maximum output amplitude; because the nonlinearity output is dimensionally an angular

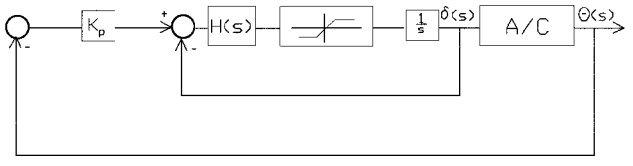

Fig. 1 Closed-loop scheme for the study of category II PIO.

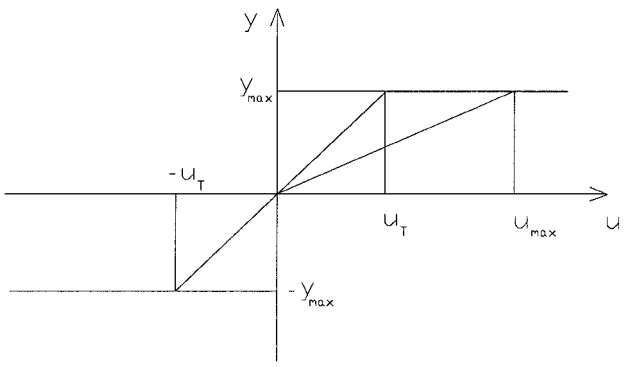

Fig. 2 Normalized nonlinear element.

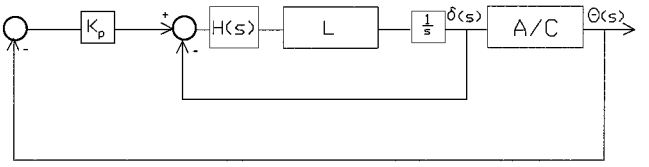

Fig. 3 Replacement of the nonlinear element with the linear gain *L*.

rate, $y_{\max}$ will be also denoted by $\dot{\delta}_{\max}$. Obviously the linear threshold in input is given by $u_T = y_{\max}$; finally $u_{\max}$ denotes the maximum input amplitude.

A classical analytical tool for general nonlinear systems is the describing function (DF) method, which is capable to reveal PIO as limit cycles of the nonlinear system. Two drawbacks exist for this method. First, the graphical nature of the classical procedure limits the extension of its applicability to the multinonlinearity case, where a basic assumption to simplify the analysis is that the nonlinear elements are independent of each other, that is, their describing functions are those obtained in the case of a single nonlinearity. Second, the numerical approach, which has been recently proposed to make full use of the computing power of modern computers, requires an a priori estimate of possible limit cycles because it is based on the solution of a nonlinear equation.

In this paper we provide two methods for PIO analysis based on the robust stability (RS) approach. To this end consider the scheme depicted in Fig. 3, where the nonlinear element has been replaced by the linear gain L. It is clear that, when the actuator is not saturated, $L = 1$ (recall that the nonlinearity has been normalized to have unitary slope); in the same way if we have an estimate of $u_{\max}$, that is the maximum input entering the nonlinear element, the minimum value attained by L is

$$L_{\min} := \begin{cases} y_{\max}/u_{\max} & \text{if} \quad u_{\max} > u_T \\ 1 & \text{if} \quad u_{\max} \leq u_T \end{cases} \tag{2}$$

therefore we can conclude that $L \in [L_{\min}, 1]$.

The second parameter that is considered in the stability analysis is the pilot gain K_p; indeed, it is well known that critical full attention maneuvers, like tracking, aerial refueling, and so forth, can require a high pilot gain, which can trigger the PIO occurrence.

The first method assumes the parameter L to be time invariant and will be shown to be equivalent, in the prediction of category II PIO, to the DF analysis method. By the replacement of the DF with the RS analysis, we will be able to exploit the tools that robust control literature has made available in the last years to deal with the stability of uncertain linear systems; moreover, (this is the object of current research) this approach can be easily extended to deal with the multinonlinear elements case and, at the same time, with actual uncertainties affecting the plant and with PIO phenomena.

The second method takes directly into account the nonlinear element, and the stability analysis is performed by means of the so-called Lur'e Lyapunov functions (see Ref. 13, Chap. 5).

Because, as it is shown in the next sections, the first method can provide an optimistic condition and the second one a conservative condition for PIO occurrence for the given aircraft, when the results obtained from the application of these conditions are close to each other a rather complete analysis of the nonlinear system can be performed. Delicate situations are those ones in which the results obtained from the conditions are discordant; in this case further investigation is necessary, for example, via time simulation analysis. The example in Sec. IV.A further clarifies this point.

III. Equivalence Between DF Analysis and RS Analysis vs a Time-Invariant Parameter

In this section we shall show how the search for limit cycles, which is the main aim of the DF analysis, is equivalent to the RS analysis of a suitable linear system.

We consider the following problem.

Problem Nonlinear (NL) (limit cycle existence): Find, if existing, the limit cycles of the closed-loop system in Fig. 1, that is, the persistent sinusoidal oscillations of the system. □

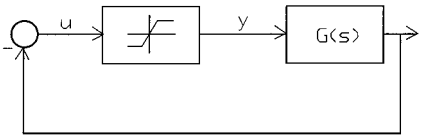

Fig. 4 Nonlinear system equivalent to the system in Fig. 1.

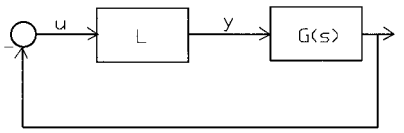

Fig. 5 Linear system obtained by replacing the nonlinear element with a gain L.

The system in Fig. 1 can be transformed into the equivalent one in Fig. 4, where $G(s)$ denotes the transfer function of the linear part of the system. By definition limit cycles are the solutions of

$$F(u)G(j\omega) = -1 \qquad F(u) \in [L_{\min}, 1] \tag{3}$$

where $F(\cdot)$ is the describing function of the nonlinearity in Fig. 2; note that $F(\cdot)$ is real, positive, and does not depend on the frequency ω.

Equation (3) can be rewritten as

$$\begin{cases} |G(j\omega)| = \dfrac{1}{|F(u)|} & F(u) \in [L_{\min}, 1] \\ \angle G(j\omega) = -180 \text{ deg} \end{cases} \tag{4}$$

If the preceding system of equations admits a solution, this gives the frequency ω of the limit cycle and the amplitude u at the input of the nonlinear element.

Next consider the following problem.

Problem Linear (LIN) $[L_{\min}, 1]$: Consider the system in Fig. 5 where the uncertain, time-invariant gain L takes values in $[L_{\min}, 1]$. Determine the range of values of L for which the closed-loop system is asymptotically stable and that for which it is not stable. For the limit values of L, determine also the neutral stability frequency, that is, the natural frequency of the closed-loop poles that are at the limit of stability. □

By a modification of the standard Nyquist Stability Theorem, the search for the stability limits can be done by inspecting the stability of the system with open-loop transfer function $G(j\omega)$ with respect to a critical point varying on the real axis of the Nyquist diagram within the range $[-1/L_{\min}, -1]$. In particular, this means that the limit values of L and the respective neutral stability frequency are the solutions of the following system of equations:

$$G(j\omega) = -1/L \qquad L \in [L_{\min}, 1] \tag{5}$$

which can be rewritten as

$$\begin{cases} |G(j\omega)| = 1/L & L \in [L_{\min}, 1] \\ \angle G(j\omega) = -180 \text{ deg} \end{cases} \tag{6}$$

By the analogy between Eqs. (4) and (6), it follows that the search for limit cycles by DF analysis and by RS analysis are equivalent for the single-loop case. In the next sections we shall provide a procedure for the RS analysis of the uncertain system depicted in Fig. 5; such a procedure will be applied to a case study to show the effectiveness of the proposed technique.

A. Procedure for RS Analysis of a Linear Time-Invariant System Subject to Uncertain Parameters

In this section we present an algorithm, ROBAN, developed at Centro Italiano Ricerche Aerospaziali (Italian Aerospace Research Center), which performs the RS analysis of a linear time-invariant (LTI) system subject to parametric time-invariant uncertainties. This algorithm can be used to solve Problem LIN $[L_{\min}, 1]$, thus allowing the detection of limit cycles in the nonlinear system in Fig. 1. The proposed algorithm is based on a polynomial approach, i.e., on the availability of the characteristic polynomial of the LTI system.

Let n be the order of the system and p the number of uncertain parameters affecting the behavior of the system itself. Let $\pi = [\pi_1, \ldots, \pi_p]^T \in \Pi \subset \mathbb{R}^p$ be the vector of uncertain parameters, ranging in the box Π, and let $\pi_0 \in \Pi$ be the vector of nominal values of the uncertain parameters.

Now let $a(\cdot): \Pi \to \mathbb{R}^n$, $\pi \mapsto a(\pi)$, the vector-valued function containing the coefficients of the characteristic polynomial of the system. Denote by $\mathcal{L}: \mathbb{R}^n \mapsto \mathbb{P}^n$, $a = (a_1 \ \cdots \ a_n)^T \mapsto p(s, a)$, where

$$p(s, a) = s^n + a_1 s^{n-1} + \cdots + a_n \qquad s \in \mathbb{C}$$

the linear operator mapping a vector of $\mathbb{R}^n$ into $\mathbb{P}^n$, the set of monic polynomials of degree n. Finally define the compound operator $\mathcal{L}_a$ as $\mathcal{L} \circ a$.

The complete behavior of the uncertain system is described by the following family of monic polynomials:

$$\mathcal{L}_a(\Pi) = \{p[\cdot, a(\pi)] \,|\, \pi \in \Pi\}$$

Definition 1: Let $\tilde{\Pi} \subseteq \Pi$; the family of polynomials $\mathcal{L}_a(\tilde{\Pi})$ is said to be Hurwitz if the roots of $p[\cdot, a(\pi)]$ are in the open left half of the complex plane for all $\pi \in \tilde{\Pi}$.

Definition 2: The stability region $\mathcal{S}$ in the parameter space Π is the set composed of all $\pi \in \Pi$ such that the roots of $p[\cdot, a(\pi)]$ are in the open left half of the complex plane.

With respect to the preceding definitions, we can pose the following problem, which is solved by ROBAN.

Problem 1: Find the stability region $\mathcal{S}$ in the parameter space Π.

As we shall see, the idea behind the algorithm ROBAN is that of approximating the stability region $\mathcal{S}$ by the union of boxes in the parameter space Π. To check robustness in the given box, it is necessary to have a procedure to solve the following basic problem.

Problem 2 (basic problem): Given a box $R \subseteq \Pi$, determine if the family of polynomials $\mathcal{L}_a(R)$ is Hurwitz.

The stability test contained in the algorithm ROBAN allows the solution of the basic problem for any kind of dependence on parameters [the only requirement is that the vector function $a(\pi)$ has to be continuous in its argument]; it implements the ideas proposed in Refs. 11, 16, and 17. We shall come back to some technical details of the stability test after the description of the algorithm.

We remark that the algorithm ROBAN computes the boundary of the stability region $\partial\mathcal{S}$ up to a desired resolution.

In the sequel we shall use the statement "the box R is Hurwitz" to mean that the family of polynomials $\mathcal{L}_a(R)$ is Hurwitz, according to Definition 1.

Procedure 1 (ROBAN):
Set the box Π in the *List*
  For each box of the *List*
    If *cond*(*box*) **then** box is Hurwitz
    Elseif $\|box\| < \varepsilon$ **then** box is not Hurwitz
    Else divide box in subboxes and update *List*
    End
  End
End of Procedure 1

After Procedure 1 has terminated, the union of the boxes for which the logical operation cond(box) is true is an approximation of the stability region $\mathcal{S}$.

Given a box R, the operation $\|R\|$ is defined as follows:

$$\|R\| = \max_{i=1,\ldots,2^p} l_i \tag{7}$$

where l_i is the ith side of the box R. In other words, the size of the box is given by the length of the longest side of the box.

The logical operation cond(R) is true if the sufficient condition for robust stability of the family of polynomials $\mathcal{L}_a(R)$, implemented via the techniques developed in Refs. 11, 16, and 17, is satisfied. For the sake of brevity, we do not detail the procedure here, but only recall the fundamental steps. First, one builds a polytope in the

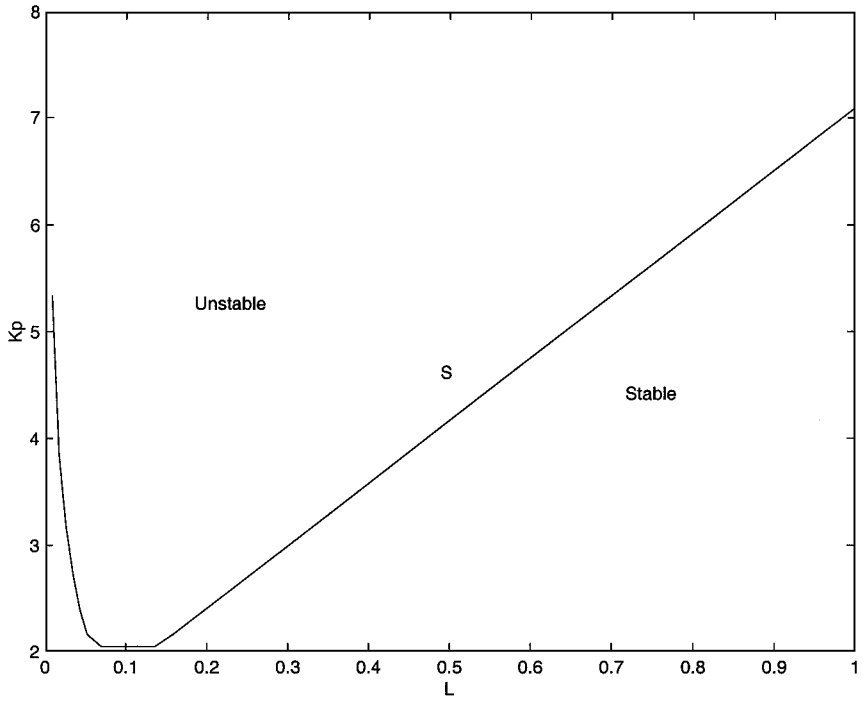

Fig. 6 Results of the stability analysis performed by ROBAN.

coefficients space $\mathbb{R}^n$, which "covers" the image of the coefficient vector over the box R, that is,

$$\mathcal{P}[a(R)] \supseteq a(R) \tag{8}$$

By virtue of Eq. (8), it readily follows that the Hurwitzness of the family of polynomials with coefficients in the set $\mathcal{P}[a(R)]$ (which is tested via the method proposed in Ref. 16) implies Hurwitzness of the original family of polynomials $\mathcal{L}_a(R)$. Moreover if the way the polytope $\mathcal{P}[a(R)]$ is constructed is such that

$$\text{Lebesgue measure of } \mathcal{P}[a(R)] \to 0 \qquad \text{as} \qquad \|R\| \to 0 \tag{9}$$

the stability region computed via Procedure 1 recovers the exact stability region $\mathcal{S}$ as the procedure parameter ε goes to zero. From a practical point of view, this means that we can estimate $\mathcal{S}$ up to the desired resolution acting on the parameter ε. Finally we remark that the covering procedure implemented in ROBAN satisfies condition (9).

B. Analysis of Limit Cycles and Their Prediction: the X-15 Case Study

In this section we will take advantage of the equivalence between DF analysis and RS analysis of linear systems in the presence of a time-invariant parameter to predict the existence of category II PIO in an aircraft with a rate-limited actuator.

Research on PIO analysis through describing function has been performed since a long time ago, and new studies have been conducted in the last years to better understand the particular problem caused by rate-limited actuators.

In Refs. 5, 15, and 18 the problem of analysis and prediction of PIO in an aircraft with actuator rate limiting is studied through DF analysis, and it is shown that this technique can be used to provide a prediction of the limit cycle or PIO frequency. Therefore we have chosen to demonstrate the capabilities of our proposed method on the same test case presented in Ref. 18, which is based on the X-15 PIO occurred on 8 June 1959 during a landing flare.[19]

The model of the aircraft with a rate-limited actuator is shown in Fig. 1; the numerical values of the elements in the block diagram are

$$\frac{\theta(s)}{\delta(s)} = \frac{3.476(s + 0.0292)(s + 0.883)}{(s^2 + 0.019s + 0.01)(s^2 + 0.8418s + 5.29)}$$

$$H(s) = \frac{1}{\tau_r} = 25\ \text{s}^{-1}$$

$$\dot{\delta}_{\max} = y_{\max} = 15\ \text{deg/s} \tag{10}$$

The equivalent linear model of the rate-limited actuator, shown in Fig. 3, can be used within the RS analysis method to derive PIO predictions.

The DF analysis predicts the following limit cycles:

1) For $K_p < 2.04$, no limit cycles exist.

2) For $K_p \in [2.04, 7.1]$, two limit cycles exist, one of which was of increasing frequency w.r.t. K_p, and the other one of decreasing frequency w.r.t. K_p.

3) For $K_p = 7.1$, two limit cycles exist, one of which, with frequency $\omega_n = 2.087$ rad/s, is a linear limit cycle, i.e., it consists of nonvanishing linear oscillations of the closed-loop system, which for this value of K_p is only marginally stable.

4) For $K_p > 7.1$, there is only one limit cycle of decreasing frequency w.r.t. K_p.

In Fig. 6 we present the results of the RS analysis performed via ROBAN with $L_{\min} = 0$. Two regions are visible in the figure, separated by a curve S. The region below S identifies the pairs of parameters (L, K_p) for which the closed-loop system is asymptotically stable (the stability region $\mathcal{S}$), whereas in the superior region the system is unstable.

On the separatrix curve S the pairs (L, K_p), for which the closed-loop system is neutrally stable, that is, a couple of poles with zero real part exists, are located. For a given K_p the neutrally stable frequencies, computed as the imaginary parts of the neutrally stable poles corresponding to the points obtained by the intersection of S with the horizontal line of ordinate K_p, are equal to the limit cycle frequency predicted by the DF analysis in total agreement with the theory of Sec. III. From Fig. 6 the power of the RS method in the prediction of limit cycles is evident. One can readily derive the existence of limit cycles with respect to a range of the pilot gain K_p. In particular, it is immediate to find the minimum K_p for the existence of limit cycles, namely, $K_p = 2.04$, the K_p for linear limit cycles, namely $K_p = 7.1$, (which is the one for which the separatrix S crosses the linear behavior curve, that is, the vertical line with $L = 1$) and the number of limit cycles for each value of K_p (which equals the number of intersection of the separatrix S with a horizontal straight line of given K_p).

C. Stability of Limit Cycles and Their Practical Occurrence

By use of informal arguments, it is possible to predict how the limit cycles found by the preceding analysis can develop in a real situation; to answer the question, refer to Fig. 7.

In the following the assumption is made that in the real situation to be analyzed the pilot gain K_p is constant, that is, it is held fixed to

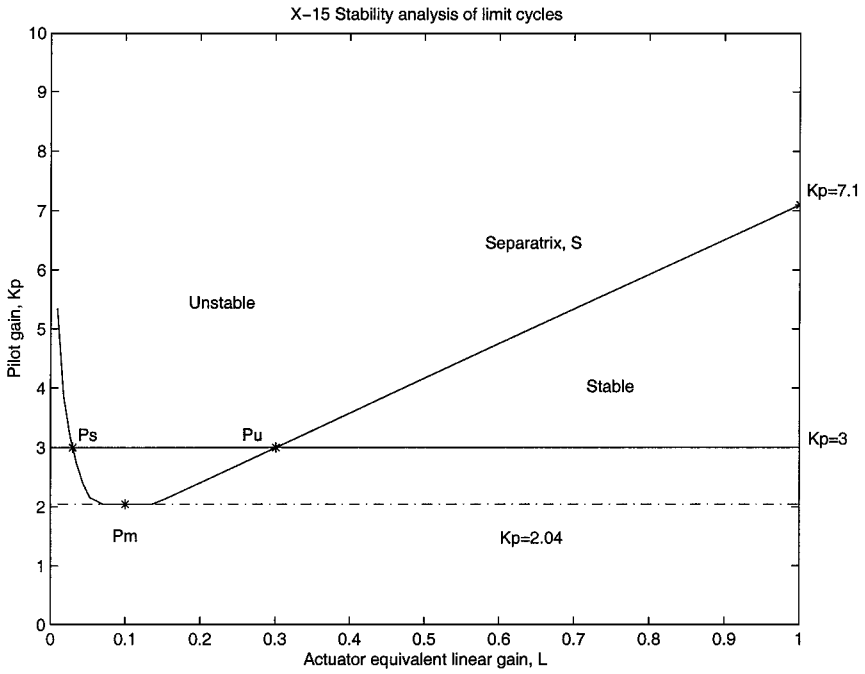

Fig. 7 Development of limit cycles.

some particular value during the maneuver, the actual value may be depending on the flight phase and the particular pilot himself. The other parameter in the figure L is on the other hand varying during the maneuver, if the actuator rate saturates (remember, however, that the analysis has been performed vs a time-invariant L; this, as said, may introduce optimism in the PIO prediction). The preceding assumptions on K_p and L mean that for a particular configuration to be analyzed one has to restrict himself to a horizontal line of given K_p. From simple considerations it is possible to establish that the points of the left branch of the boundary line S between stable and unstable regions, up to the minimum point $(L, K_p) \cong (0.15, 2.04)$, are points of stable limit cycles (for the definition of stable and unstable limit cycles see Ref. 13, Chap. 1). On the other hand, the points of the right branch of the separatrix S are associated with unstable limit cycles. To justify this claim, let us analyze the behavior in a neighboring of a limit cycle, i.e., close to the separatrix S of Fig. 7.

Moving on a horizontal line of given K_p (=3 in Fig. 7) greater than the minimum K_p of the points of S (=2.04 in Fig. 7), two different situations are possible:

1) By increasing L, we move from a stable region to an unstable region. This is the situation of all of the points on the left part of the boundary S, for example, P_s, up to the point of minimum K_p. Limit cycles on this part of the boundary are stable limit cycles. Indeed, starting from P_s, when one moves from left to right on the horizontal line the instantaneous gain of the saturation is increased, but, because the output is fixed to the saturation value, this means that the amplitude of the input is decreased. Because L has now moved into the unstable region, the system is now unstable, and the amplitude of the oscillations tends to increase, recovering the initial situation. On the other hand, if L decreases the input to the nonlinear element is first increasing, but then, because of the asymptotical stability of the system in the new situation, it will finally decrease until P_s is reached again. This motivates our definition of a stable limit cycle in P_s.

2) Based on similar considerations, the limit cycle in the point P_u can be classified as an unstable one.

From this the following behaviors of the complete system are predicted:

1) For $K_p < 2.04$ the linear system ($L = 1$) is stable, and no intersection with the separatrix S (no limit cycle) is detected. Therefore in this case no limit cycles will occur, and the origin of the system state is asymptotically stable. This means that even if rate saturation occurs during the maneuver it will not develop in a limit cycle but the actuator will exit from the rate-limiting situation, and the system will settle to its linear equilibrium point.

2) For $K_p \in [2.04, 7.1]$ the linear system ($L = 1$) is asymptotically stable, and, moving toward left on the horizontal line at constant K_p, two limit cycles are met: first an unstable limit cycle (the point P_u in the figure), then a stable limit cycle (the point P_s in the figure). We now remind that decreasing L means that the input to the saturation element is increasing, and in our case the input to the saturation is the demanded rate of the actuator deflection. Therefore the conclusion can be made that two behaviors are possible, depending on the amplitude of the rate demanded to the actuator:

a) First, as far as the system will demand a low actuation rate, the system is stable, and the equilibrium point is the linear one. Therefore no limit cycle develops if the demanded rate is low.

b) When the demanded rate is higher than the one corresponding to the unstable limit cycle, then an unstable behavior develops, which leads the system to the working point on the second limit cycle—the one on the left side of the separatrix, which is a stable limit cycle. Therefore in the end the system will settle to this limit cycle for a high demanded rate.

3) For $K_p > 7.1$ the linear system is unstable, and there exists only one limit cycle, which is a stable one. Therefore in this case the steady-state behavior of the system is always a limit cycle.

Finally, a set of time simulations of the nonlinear model (i.e., with the actual saturation block instead of the equivalent linear gain L) has been run. The set of simulations includes both step responses with different step amplitudes and zero input responses with different values of initial conditions of the actuator deflection and the aircraft pitch attitude angle. For each time simulation different values of the pilot gain K_p have been used, and the frequency of the resulting limit cycle has been recorded. Figure 8 shows the pitch attitude responses to a doublet command for two values of the pilot gain. The continuous and dashed lines are obtained for pilot gains equal to two and three, respectively; according to RS analysis for $K_p = 3$, a limit cycle occurs.

Time simulations show that the frequency of the occurred limit cycles is independent of the amplitude of the step input and of the given initial condition and only depends on the value of the pilot gain; in other words, the same limit cycle frequency results in all of the simulations having the same value of the pilot gain.

In Fig. 9 the values of the limit cycle frequencies obtained by the use of RS (or equivalently DF) analysis and the time simulations

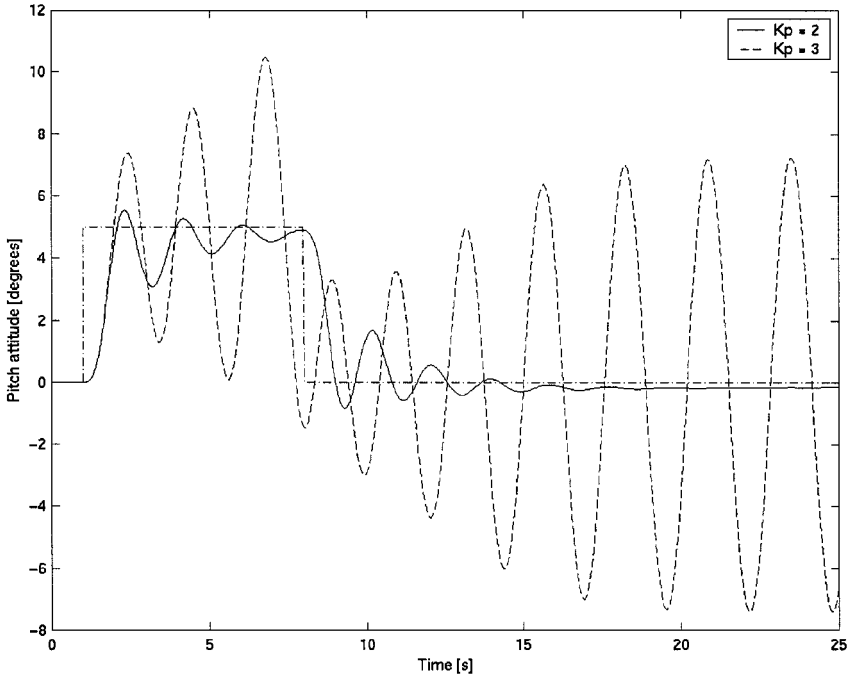

Fig. 8 Pitch attitude responses to doublet commands for different values of the pilot gain K_p.

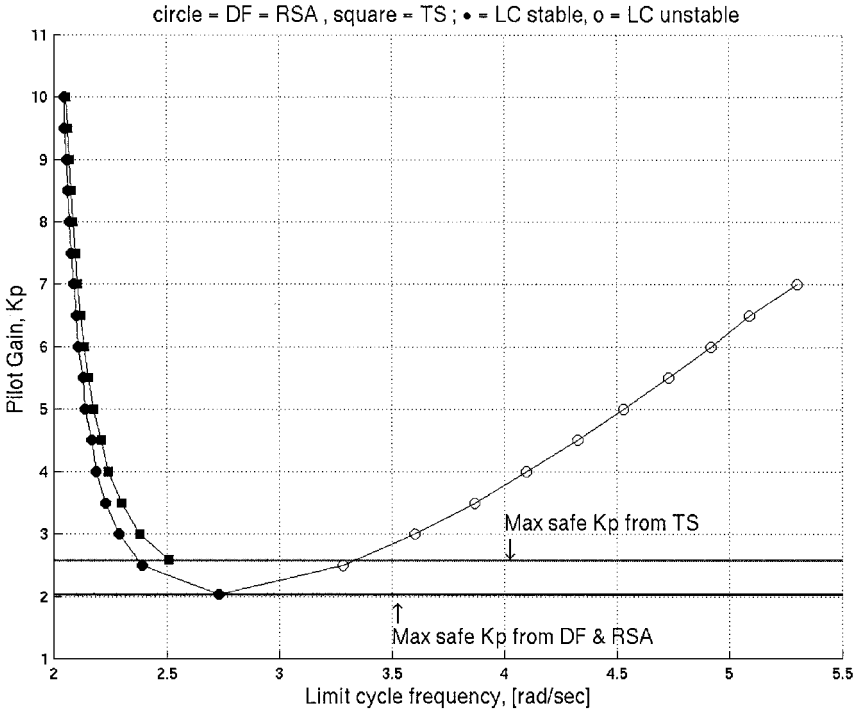

Fig. 9 Comparison of limit cycle frequency predicted by 1) DF analysis, 2) RSA, and 3) time simulations (TS) of the Simulink nonlinear model.

method are shown. The limit cycle frequencies determined via simulations are very close to those ones determined via RS (DF) analysis; this confirms the goodness of the proposed analysis method.

A further comment can be derived from Fig. 9; the curve of the limit cycle frequencies from time simulations does only have a decreasing part in the left side of the plot, whereas the curve from RS (DF) analysis does have both a decreasing part and an increasing part at the right of a frequency of about 2.74 rad/s. The two branches correspond respectively to the stable limit cycles and the unstable limit cycles, which are predicted for the range of pilot gain $K_p = [2.04, 7.1]$. It is therefore clear why the time simulation analysis does not have the increasing branch on the right side: it is representative of unstable limit cycles, which cannot be detected in a real world nonlinear simulation environment.

IV. Stability Analysis Using the Popov Approach

If we try to infer stability of the nonlinear system in Fig. 1 (or equivalently Fig. 4) from the analysis of the linear scheme in Fig. 3 (or equivalently Fig. 5), the result can be fallacious; indeed the input-output gain of the nonlinear element in Fig. 2 is time varying, whereas the stability analysis performed in the preceding section assumes that the gain L is time invariant. Because stability vs a time-invariant parameter does not guarantee stability vs a time-varying parameter (see Ref. 13, Chap. 4), the approaches based on both DF

and RS analysis may be optimistic in predicting the existence of PIO for a given aircraft.

A possible way to validate RS analysis is that of performing extensive simulations of the nonlinear system, according to Sec. III.C; however, this approach may be extremely time consuming. An alternative simple analytical method is proposed in this section; this method leads to a sufficient (conservative) condition for asymptotic stability of the original nonlinear system.

Actually we can consider two different approaches to analyze the stability properties of the nonlinear system in Fig. 4, both leading to a sufficient condition for asymptotic stability: 1) to replace the nonlinear element in Fig. 4 with a time-varying gain $L(t) \in [L_{\min}, 1]$ and check robust stability of the resulting closed-loop uncertain linear system; and 2) to analyze directly the stability properties of the nonlinear system in Fig. 4.

In case 1) we can use the so-called quadratic stability (QS) approach (see Ref. 20); such a classical method makes use of a quadratic Lyapunov function in the form

$$V(x) = x^T P x \tag{11}$$

with P positive definite; if there exists a P such that the derivative of V along the solutions of the linear system in Fig. 5 is negative definite for all $L \in [L_{\min}, 1]$, then it is guaranteed asymptotic stability of the same system for all time-varying realizations of the gain L in $[L_{\min}, 1]$ and therefore also asymptotic stability of the nonlinear system in Fig. 4.

In general, the QS approach is a conservative analysis tool because, as said, it guarantees stability with respect to all possible time-varying behaviors of L and hence also for unrealistically fast variation of the gain (in our case this conservatism has been confirmed by the application of the QS approach to the X-15 case[21]).

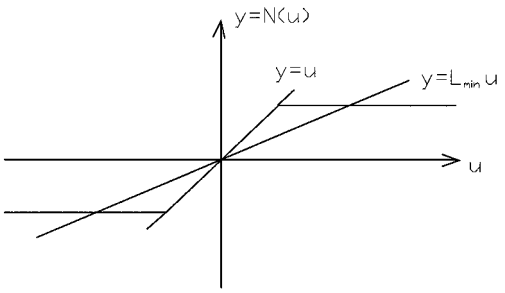

Fig. 10 Nonlinearity sector.

To follow the approach suggested at point 2), let us refer to Fig. 4 and denote by (A, B, C) a state-space realization of the transfer function $G(s)$; we have

$$\dot{x} = Ax + By \tag{12a}$$

$$u = -Cx \tag{12b}$$

$$y = N(u) \tag{12c}$$

The nonlinearity satisfies the sector condition (Fig. 10)

$$L_{\min} u^2 \leq uN(u) \leq u^2 \tag{13}$$

The sector condition (13) can be reduced to a standard one by means of the loop transformation

$$\bar{N}(u) = 1/(1 - L_{\min})[N(u) - L_{\min} u] \tag{14}$$

Indeed $\bar{N}$ satisfies

$$0 \leq u\bar{N}(u) \leq u^2 \tag{15}$$

Substitution of Eq. (14) into Eq. (12) leads to the Lur'e system

$$\dot{x} = (A - BCL_{\min})x + B(1 - L_{\min})y := \bar{A}x + \bar{B}y \tag{16a}$$

$$u = -Cx \tag{16b}$$

$$y = \bar{N}(u) \tag{16c}$$

subject to the standard sector condition (15).

Obviously asymptotic stability of the nonlinear system (15) and (16) is equivalent to asymptotic stability of the original system (12) and (13).

A sufficient condition for the stability of Eqs. (15) and (16) can be found by using the Lur'e type Lyapunov function (see Ref. 13, Chap. 5)

$$V(x) = x^T P x + 2\lambda \int_0^{Cx} \bar{N}(u)\, \mathrm{d}u \tag{17}$$

where P is a positive definite matrix and λ is a nonnegative scalar. The function (17) recovers as a particular case ($\lambda = 0$) the Lyapunov

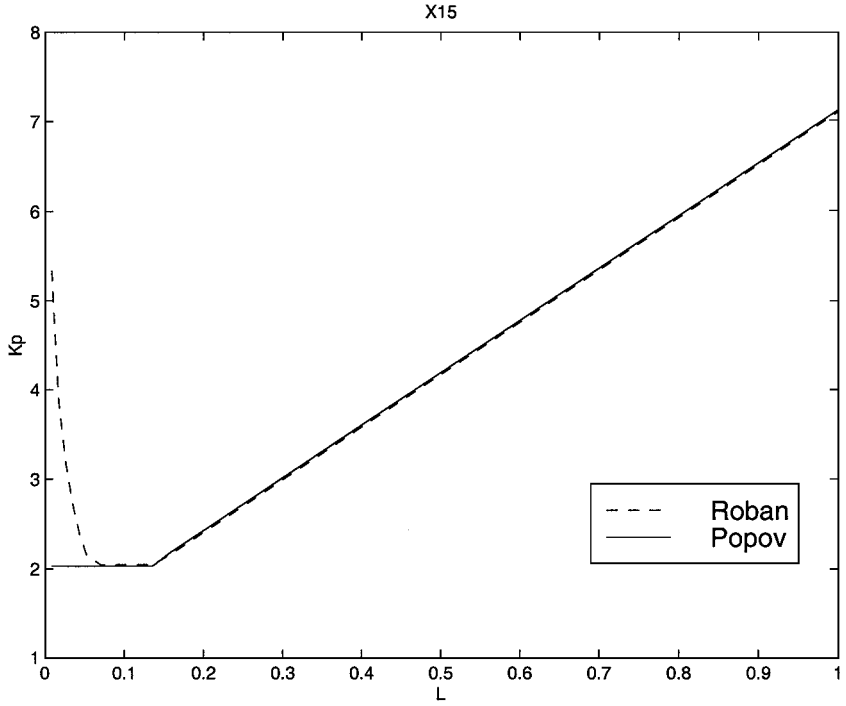

Fig. 11 X-15: The boundaries of the stability region evaluated via ROBAN (– – –) and Popov (——).

function (11); from this observation it immediately follows that the approach suggested at point 2) is less conservative than the QS approach.

If there exist P and λ such that the derivative of $V(\cdot)$ along the trajectories of system (15) and (16) is negative definite, the same system is asymptotically stable. Such a condition can be converted into a linear matrix inequality (LMI) as shown in Ref. 22, Chap. 8; this result is summarized in the following theorem (known as the Popov Criterion).

Theorem 1 Popov Criterion—LMI version[22]: System (15) and (16) is asymptotically stable if there exists a positive definite matrix P and nonnegative scalars λ, τ such that the following LMI is satisfied:

$$\begin{pmatrix} \bar{A}^T P + P\bar{A} & P\bar{B} - \bar{A}^T C^T \lambda - C^T \tau \\ \bar{B}^T P - \lambda C\bar{A} - \tau C & -\lambda C\bar{B} - \bar{B}^T C^T \lambda - 2\tau \end{pmatrix} < 0 \qquad (18)$$

□

Theorem 1 leads to an LMI-based feasibility problem, which, if admitting a solution, guarantees asymptotic stability of the nonlinear system in Fig. 4. Commercial software is available for solving LMI problems (see for example the MATLAB® LMI Control Toolbox[23]).

To make a comparison between the RS analysis considered in Sec. III and the stability analysis via the Popov Criterion, we have again considered the X-15 PIO test case. We have applied the theory of Sec. IV to estimate, for several values of $L_{\min}$ between 0 and 1, the maximum value of K_p, which does not destabilize the system, say $\hat{K}_p(L_{\min})$. Then we have considered the boundary of the stability region obtained by joining the values $\hat{K}_p(L_{\min})$ for $L_{\min} \in (0, 1]$.

In Fig. 11 we have depicted the Popov stability region (limited by the continuous line) together with the stability region evaluated by ROBAN (limited by the dashed line).

As said before, the ROBAN approach may be optimistic, whereas the Popov approach may be conservative; in the case considered here, however, the stability boundary obtained by the Popov method is practically coincident with the one obtained via the ROBAN method {in the sense that, for a given K_p, the stability interval over the L axis $[L_{\min}(K_p), 1]$ [The number $L_{\min}(K_p)$ is defined as the maximum between the abscissae of the pair of points obtained via the intersection of the stability boundary with the horizontal line of ordinate K_p.] is the same for both ROBAN and Popov}. Therefore the Popov approach validates the ROBAN approach for the X-15 case.

This example shows how the combined use of the ROBAN and the Popov approaches allows a rather complete analysis of category II PIO for a given aircraft. Delicate situations are those ones in which the stability boundaries, obtained by the two approaches, are sensibly different; in this case further investigation is necessary (for instance via time-simulation analysis) to gain more insights about the case under consideration.

V. Conclusions

In this paper we have provided two analytical methods for the analysis of category II PIO. The first method works by replacing the nonlinear actuator by a linear, uncertain, time-invariant gain. The linear fictitious system is then analyzed via a robust stability analysis approach based on the use of the software ROBAN developed at Centro Italiano Ricerche Aerospaziali; this approach has been shown to be equivalent, in the prediction of category II PIO, to the DF analysis method. However the robust stability analysis is easier to perform; it allows one to deal, at the same time, with actual uncertainties affecting the plant and with PIO phenomena and (this is the object of current research) can be extended to deal with the multi-nonlinear elements case.

Because the method based on robust stability analysis can be optimistic in predicting the existence of PIO for a given aircraft, it is necessary to validate the results obtained by this approach. A possible way to do this is to perform exhaustive time simulations of the nonlinear system; obviously time simulations can reveal to be extremely time consuming.

Based on the preceding consideration, a further simple analytical method has been proposed. Such a method (namely the Popov approach) takes directly into account the nonlinear element, and the stability analysis is performed by means of the so-called Lur'e Lyapunov functions. Because the first method can be optimistic and the second one conservative, by the use of both methods a complete analysis of the nonlinear system can be performed; time simulations become necessary only when there is discordance between the two analytical methods.

Finally, the goodness of the proposed methods has been tested on the X-15 case study.

References

[1]McRuer, D. T., Droste, C. S., Hansman, R. J., Hess, R. A., Lemaster, D. P., Matthews, S., McDonnell, J. D., McWha, J., Melvin, W. W., and Pew, R. W., *Aviation Safety and Pilot Control. Understanding and Preventing Unfavorable Pilot-Vehicle Interactions*, ASEB National Research Council, National Academy Press, Washington, DC, 1997.

[2]Military Specification, "Flying Qualities of Piloted Airplanes," MIL-F-8785 C, Wright–Patterson AFB, OH, Nov. 1980.

[3]Military Standard, "Flying Qualities of Piloted Aircraft," MIL-STD-1797 A, Wright–Patterson AFB, OH, Jan. 1990.

[4]Mitchell, D., Hoh, R., Aponso, B., and Klyde, D., "Proposed Incorporation of Mission-Oriented Flying Qualities into MIL STD-1797A," Wright Lab., WL-TR-95-3049, Wright–Patterson AFB, OH, Oct. 1994.

[5]Klyde, D. H., McRuer, D. T., and Myers, T. T., "Unified Pilot-Induced Oscillation Theory, Volume I: PIO Analysis with Linear and Nonlinear Effective Vehicle Characteristics, Including Rate Limiting," Wright Lab., WL-TR-96-3028, Wright–Patterson AFB, OH, Jan.–Feb. 1995.

[6]Anderson, M. R., and Page, A. B., "Unified Pilot-Induced Oscillation Theory, Volume III: PIO Analysis Using Multivariable Methods," Wright Lab., WL-TR-96-3030, Wright–Patterson AFB, OH, Dec. 1995.

[7]Duda, H., "Minutes on a Workshop on Pilot-in-the-Loop Oscillations held at DLR, Braunschweig on June 12, 13th, 1997," DLR, IB 111-97/25, Brunswick, Germany, June 1997.

[8]Duda, H., "Prediction of Pilot-in-the-Loop Oscillations due to Rate Saturation," *Journal of Guidance, Control, and Dynamics*, Vol. 20, No. 3, 1997, pp. 581–587.

[9]Bailey, R. E., and Bidlack, T. J., "Unified Pilot-Induced Oscillation Theory, Volume IV: Time Domain Neal-Smith Criterion," Wright Lab., WL-TR-96-3031, Wright–Patterson AFB, OH, Dec. 1995.

[10]Verde, L., "Controllo Robusto di Aeromobili: Metodi Parametrici per l'Analisi e la Sintesi," Ph.D. Dissertation, Dept. of Information Systems, Univ. of Naples, Feb. 1992 (in Italian).

[11]Cavallo, A., De Maria, G., and Verde, L., "Robust Flight Control Systems: a Parameter Space Design," *Journal of Guidance, Control, and Dynamics*, Vol. 15, No. 5, 1992, pp. 1207–1215.

[12]Cavallo, A., De Maria, G., and Verde, L., "Robust Analysis of Handling Qualities in Aerospace Systems," *Proceedings of the 11th IFAC World Congress*, Vol. 5, Elsevier, Amsterdam, 1990, pp. 70–75.

[13]Khalil, K. H., *Nonlinear Systems*, MacMillan, New York, 1992.

[14]Amato, F., Iervolino, R., Scala, S., and Verde, L., "New Criteria for the Analysis of PIO Based on Robust Stability Methods," *Proceedings of the AIAA Atmospheric Flight Mechanics Conference*, AIAA, Reston, VA, 1999, pp 31–48.

[15]McRuer, D., "Pilot-Induced Oscillations and Human Dynamic Behaviour," NASA CR 4683, July 1995.

[16]Cavallo, A., Celentano, G., and De Maria, G., "Robust Stability Analysis of Polynomials with Linearly Dependent Coefficient Perturbations," *IEEE Transactions on Automatic Control*, Vol. 36, No. 3, 1991, pp. 380–384.

[17]Amato, F., Garofalo, F., Glielmo, L., and Verde, L., "An Algorithm to Cover the Image of a Function with a Polytope: Applications to Robust Stability Problems," *Proceedings of the IFAC World Congress*, Vol. 6, Institution of Engineers, Barton, Australia, 1993, pp. 423–427.

[18]Klyde, D. H., McRuer, D. T., and Myers, T. T., "Pilot-Induced Oscillation Analysis and Prediction with Actuator Rate Limiting," *Journal of Guidance, Control, and Dynamics*, Vol. 20, No. 1, 1997, pp. 81–89.

[19]Matranga, G. J., "Analysis of X-15 Landing Approach and Flare Characteristics Determined from the First 30 Flights," NASA TN D-1057, July 1961.

[20]Barmish, B. R., " Stabilization of Uncertain Systems via Linear Control," *IEEE Transactions on Automatic Control*, Vol. 28, No. 6, 1983, pp. 848–850.

[21]Amato, F., Iervolino, R., Scala, S., and Verde, L., "Prediction of Category II Pilot in the Loop Oscillations (PIO) via Robust Stability Analysis," Centro Italiano Recerche Aerospaziali, CIRA-TR-98-203, Capua, Italy, Dec. 1998.

[22]Boyd, M., El Ghaoui, L., Feron, E., and Balakrishnan, V., *Linear Matrix Inequalities in System and Control Theory*, Society for Industrial and Applied Mathematics Press, Philadelphia, 1993.

[23]Gahinet, P., Nemirovski A., Laub, A. J., and Chilali, M., *LMI Control Toolbox*, Mathworks, Inc., Natick, MA, 1995.